

Si–H Activation in Titanocene and Zirconocene Complexes of Alkynylsilanes $\text{RC}\equiv\text{CSiMe}_2\text{H}$ ($\text{R} = t\text{Bu}, \text{Ph}, \text{SiMe}_3, \text{SiMe}_2\text{H}$): A Model To Understand Catalytic Reactions of Hydrosilanes**

Normen Peulecke, Andreas Ohff, Peer Kosse, Annegret Tillack, Anke Spannenberg, Rhett Kempe, Wolfgang Baumann,* Vladimir V. Burlakov and Uwe Rosenthal*

Dedicated to Professor Carl Krüger on the occasion of his 65th birthday.

Abstract: The acetylene exchange in $[\text{L}_2\text{Ti}(\eta^2\text{-Me}_3\text{SiC}_2\text{SiMe}_3)]$ ($\text{L} = \text{Cp}$ ($\eta^5\text{-C}_5\text{H}_5$), Cp^* ($\eta^5\text{-C}_5\text{Me}_5$), THI ($\eta^5\text{-tetrahydroindenyl}$), $\text{L}_2 = \text{Me}_2\text{Si}(\eta^5\text{-C}_5\text{H}_4)_2$) by corresponding alkynylsilanes $\text{RC}\equiv\text{CSiMe}_2\text{H}$ or, alternatively, the reduction of $[\text{L}_2\text{TiCl}_2]$ with magnesium in THF in the presence of alkynylsilanes led to the formation of titanocene silylalkyne complexes $[\text{L}_2\text{Ti}(\text{RC}_2\text{SiMe}_2\text{H})]$; $\text{L} = \text{Cp}$, $\text{R} = t\text{Bu}$ **1**, **Ph** **2**, SiMe_3 **3**, SiMe_2H **4**; $\text{L} = \text{Cp}^*$, $\text{R} = t\text{Bu}$ **5**, $\text{R} = \text{SiMe}_2\text{H}$ **6**; $\text{L} = \text{THI}$, $\text{R} = t\text{Bu}$ **7** and $\text{L}_2 = \text{Me}_2\text{Si}(\eta^5\text{-C}_5\text{H}_4)_2$, $\text{R} = t\text{Bu}$ **8**. The zirconocene alkyne complexes with additional ligands $[\text{Cp}_2\text{Zr}(\text{thf})(\eta^2\text{-RC}_2\text{SiMe}_2\text{H})]$; $\text{R} = t\text{Bu}$ **9a**, **Ph** **10a**, SiMe_3 **11a**, and SiMe_2H **12a** were also prepared by an acetylene exchange reaction starting from $[\text{Cp}_2\text{Zr}(\text{thf})(\eta^2\text{-Me}_3\text{SiC}_2\text{SiMe}_3)]$ and the corresponding

alkynylsilanes $\text{RC}\equiv\text{CSiMe}_2\text{H}$. Dynamic NMR investigations in $[\text{D}_8]\text{THF}$ show an equilibrium between $[\text{Cp}_2\text{Zr}(\text{thf})(\eta^2\text{-RC}_2\text{SiMe}_2\text{H})]$ and the solvent-free derivative $[\text{Cp}_2\text{Zr}(\text{RC}_2\text{SiMe}_2\text{H})]$. Upon dissolving in *n*-hexane a complete elimination of the THF ligand yields zirconocene alkyne complexes without additional ligands $[\text{Cp}_2\text{Zr}(\text{RC}_2\text{SiMe}_2\text{H})]$; $\text{R} = t\text{Bu}$ **9b**, **Ph** **10b**, SiMe_3 **11b**, and SiMe_2H **12b**. IR spectra, X-ray structural, and NMR investigations indicate that the characteristic feature of the titanocene complexes **1–4** and **8** and the zirconocene complexes without THF ligands **9b–12b** is an agostic interaction

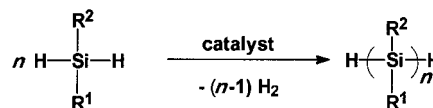
Keywords: homogeneous catalysis · Si ligands · Si–H activation · titanium · zirconium

between the Si–H bond and the metal center. The effect of this Si–H–metal interaction is considerably stronger at low temperatures and in the solid state. The L_2M moieties showing this bond activation are active catalysts in hydrosilylation and dehydrogenative polysilylation formation reactions. In the case of $\text{PhC}\equiv\text{CSiMe}_2\text{H}$ a coupling of two acetylenes to give titana- (**13**) and zirconacyclopentadienes (**14**) was observed; the unsymmetrically substituted compounds **13a**, **14a** are kinetically favored and formed first. Subsequent cycloreversion leads to the thermodynamically more stable symmetrical metallacyclopentadienes **13b** and **14b**. Both compounds do not show any interaction of the Si–H groups with the metal.

Introduction

Extensive investigations of polysilanes has resulted in a number of potential applications as advanced materials.^[1] The general method for the preparation of polysilanes is the Wurtz-type coupling of dichlorosilanes by alkali metals.^[2] An

alternative method is the transition-metal-catalyzed dehydrogenative coupling of silanes (Scheme 1).



Scheme 1. The dehydrogenative coupling of silanes as a synthetic route to polysilanes.

In 1985 Harrod et. al obtained for the first time polysilane chains of significant length (10–20 Si atoms) by this method in the presence of Group 4 metallocene compounds.^[3] Since metallocenes proved to be particularly efficient in the coupling reaction, several types of catalyst precursors have been successfully tested by different research groups: L_2MR_2 ($\text{L} = \text{Cp}, \text{Cp}^*$; $\text{M} = \text{Ti}, \text{Zr}$; $\text{R} = \text{Me}, \text{Ph}$) by Harrod and co-

[*] Dr. W. Baumann,* Prof. Dr. U. Rosenthal,* Dr. N. Peulecke, Dr. A. Ohff, Dr. P. Kosse, Dr. A. Tillack, Dr. A. Spannenberg, Dr. R. Kempe, Dr. V. V. Burlakov
Institut für Organische Katalyseforschung an der Universität Rostock e. V.
Buchbinderstrasse 5–6, D-18055 Rostock (Germany)
Fax: (+49) 381-466-93-86
E-mail: urosen@chemie1.uni-rostock.de

[**] Supporting information for this article is available on the WWW under <http://www.wiley-vch.de/home/chemistry/> or from the author. This contains tables with temperature-dependent NMR data of complexes **1**, **4**, **8**, **10**, **11**, **12**, and **14**.

workers, $[\text{CpCp}^*\text{M}[\text{Si}(\text{SiMe}_3)_3]\text{R}]$ ($\text{M} = \text{Zr}, \text{Hf}; \text{R} = \text{H}, \text{Cl}, \text{Me}$) by Tilley and co-workers,^[4] combinations of $[\text{Cp}_2\text{MCl}_2]$ ($\text{M} = \text{Ti}, \text{Zr}, \text{Hf}$) or $[\text{Me}_2\text{E}(\text{C}_5\text{H}_4)_2\text{MCl}_2]$ ($\text{E} = \text{Si}, \text{C}; \text{M} = \text{Ti}, \text{Zr}, \text{Hf}$) with $n\text{BuLi}$ by Corey and co-workers,^[5] and $[\text{Cp}_2\text{M}(\text{OAr})_2]$ ($\text{M} = \text{Ti}, \text{Zr}$) by Corriu and Moreau.^[6]

The mechanism of the dehydrogenative polymerization of silanes is still under investigation, but there are two main proposals regarding possible intermediates. A postulated mechanism by Tilley suggests a stepwise σ -bond metathesis, which involves four-center transition states.^[7] A second mechanism suggested includes metallasilylene intermediates as catalytically active species, whereas Hengge and Weinberger proposed a β -elimination from $[\text{L}_2\text{M}(\text{H})(\text{SiR}_2-\text{SiR}_3)]$ yielding $[\text{L}_2\text{M}=\text{SiR}_2]$ and HSiR_3 .^[8] Harrod for his part favored an α -elimination of hydrogen from $[\text{L}_2\text{M}(\text{H})\text{SiHR}_2]$ for the formation of $[\text{L}_2\text{M}=\text{SiR}_2]$.^[9]

Abstract in German: Der Alkin-Austausch in $[\text{L}_2\text{Ti}(\eta^2\text{-Me}_3\text{-SiC}_2\text{SiMe}_3)]$ ($\text{L} = \text{Cp}$ ($\eta^5\text{-C}_5\text{H}_5$), Cp^* ($\eta^5\text{-C}_5\text{Me}_5$), THI ($\eta^5\text{-Tetrahydroindenyl}$), $\text{L}_2 = \text{Me}_2\text{Si}(\eta^5\text{-C}_5\text{H}_4)_2$) durch entsprechende Alkynylsilane $\text{RC}\equiv\text{CSiMe}_2\text{H}$ oder alternativ die Reduktion von $[\text{L}_2\text{TiCl}_2]$ mit Magnesium in THF bei Anwesenheit der Alkynylsilane führt zur Bildung der Titanocen-Silylalkin-Komplexe $[\text{L}_2\text{Ti}(\text{RC}_2\text{SiMe}_2\text{H})]$; $\text{L} = \text{Cp}$, $\text{R} = t\text{Bu}$ **1**, **Ph** **2**, SiMe_3 **3**, SiMe_2H **4**; $\text{L} = \text{Cp}^*$, $\text{R} = t\text{Bu}$ **5**, $\text{R} = \text{SiMe}_2\text{H}$ **6**; $\text{L} = \text{THI}$, $\text{R} = t\text{Bu}$ **7** und $\text{L}_2 = \text{Me}_2\text{Si}(\eta^5\text{-C}_5\text{H}_4)_2$, $\text{R} = t\text{Bu}$ **8**. Die analogen Zirconocen-Komplexe mit Zusatzliganden $[\text{Cp}_2\text{Zr}(\text{thf})(\eta^2\text{-RC}_2\text{SiMe}_2\text{H})]$; $\text{R} = t\text{Bu}$ **9a**, **Ph** **10a**, SiMe_3 **11a** und SiMe_2H **12a** wurden ausgehend vom $[\text{Cp}_2\text{Zr}(\text{thf})(\eta^2\text{-Me}_3\text{-SiC}_2\text{SiMe}_3)]$ ebenfalls über einen Alkin-Austausch durch die Alkynylsilane $\text{RC}\equiv\text{CSiMe}_2\text{H}$ hergestellt. Dynamische NMR-Untersuchungen in $[\text{D}_8]\text{THF}$ zeigen ein Gleichgewicht zwischen $[\text{Cp}_2\text{Zr}(\text{thf})(\eta^2\text{-RC}_2\text{SiMe}_2\text{H})]$ und dem Lösungsmittel-freien Derivat $[\text{Cp}_2\text{Zr}(\text{RC}_2\text{SiMe}_2\text{H})]$. Beim Auflösen in *n*-Hexan tritt eine völlige Eliminierung des THF-Liganden ein, und die Zirconocen-Alkin-Komplexe ohne Zusatzliganden $[\text{Cp}_2\text{Zr}(\text{RC}_2\text{SiMe}_2\text{H})]$; $\text{R} = t\text{Bu}$ **9b**, **Ph** **10b**, SiMe_3 **11b** und SiMe_2H **12b** fallen an. Das wichtigste Merkmal der Titanocen-Komplexe **1-4** und **8** sowie der Zirconocen-Komplexe ohne THF Liganden **9b-12b** ist eine agostische Wechselwirkung zwischen den Si-H-Bindungen und dem Metallzentrum, die in den IR-Spektren, den Röntgenkristallstrukturen und NMR-Untersuchungen angezeigt wird. Der Effekt der Si-H-Metall-Wechselwirkung ist im Festzustand und bei tiefen Temperaturen beträchtlich stärker ausgeprägt. Die L_2M -Komplexe, die eine solche Bindungs-Aktivierung zeigen, sind auch die aktivsten Katalysatoren bei der Hydrosilylierung und der dehydrierenden Bildung von Polysilanen. Im Falle des $\text{PhC}\equiv\text{CSiMe}_2\text{H}$ kuppeln zwei Acetylene zu Titanacyclopentadienen (**13**) und Zirconacyclopentadienen (**14**), wobei die Bildung der unsymmetrisch substituierten Verbindungen **13a**, **14a** kinetisch begünstigt ist und zuerst erfolgt. Eine anschließende Cycloreversion führt zu den thermodynamisch stabileren und symmetrisch substituierten Metallacyclopentadienen **13b** und **14b**. Beide Verbindungen zeigen keine Wechselwirkung der Si-H-Gruppen mit dem Metall.

The stereoselective dehydrogenative polymerization of phenylsilane has also been investigated.^[10] In all catalytic polymerizations of silanes the complexation and activation of a Si–H bond is the most important elemental step. In this respect this bonding, starting from a very weak interaction up to a Si–H bond cleavage has been intensively studied.^[11] In most cases saturated alkyl- or arylsilanes were studied; however, little interest has been focused on the unsaturated alkynylsilanes.

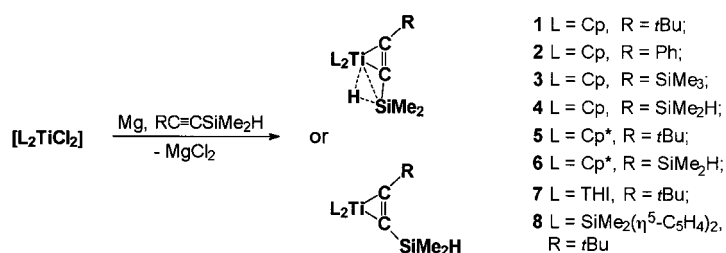
Eaborn et al. reported the oxidative addition of a Si–H group in $\text{HMe}_2\text{SiC}\equiv\text{CSiMe}_2\text{H}$ to Pt^0 in preference to the π -coordination of the triple bond, this led to the complex $\text{cis-}[\text{Pt}(\text{H})\text{SiMe}_2\text{C}\equiv\text{CSiMe}_2\text{H}(\text{PPh}_3)_2]$.^[12] Reactions of alkynylsilanes with cobalt carbonyl complexes have also been described.^[13]

Recently, we reported the reaction of the *cis*-alkyne complex $[\text{Cp}_2\text{Ti}(\eta^2\text{-Me}_3\text{-SiC}_2\text{SiMe}_3)]$ with $t\text{BuC}\equiv\text{CSiMe}_2\text{H}$ which gave the *trans*-alkyne complex $[\text{Cp}_2\text{Ti}(t\text{BuC}\equiv\text{CSiMe}_2\text{H})]$ with a strong Si–H–Ti interaction.^[14] Ab initio calculations on this complex suggest a better formulation as a d^2 metal compound with a strong σ^* -accepting H–Si bond.^[15] In catalytic investigations titanocene alkyne complexes $[\text{L}_2\text{Ti}(\eta^2\text{-Me}_3\text{-SiC}_2\text{SiMe}_3)]$ ($\text{L} = \eta^5\text{-C}_5\text{H}_5$, $\eta^5\text{-C}_5\text{Me}_5$, $\eta^5\text{-tetrahydroindenyl}$, $\text{Me}_2\text{Si}(\eta^5\text{-C}_5\text{H}_4)_2$, $(\text{O})(\text{Me}_2\text{Si})_2(\eta^5\text{-C}_5\text{H}_4)_2$) and the zirconocene alkyne complexes $[\text{Cp}_2\text{Zr}(\text{thf})(\eta^2\text{-Me}_3\text{-SiC}_2\text{SiMe}_3)]$ and $[\text{Cp}_2\text{Zr}(\text{pyridine})(\eta^2\text{-Me}_3\text{-SiC}_2\text{SiMe}_3)]$ were found to be effective precatalysts in dehydrogenative silane polymerization.^[17] This demonstrates the particular affinity of Group 4 metallocenes toward Si–H bonds.^[16] Herein we report reactions of titanocene and zirconocene derivatives with alkynylsilanes and discuss the character of the resulting Si–H metal interactions.

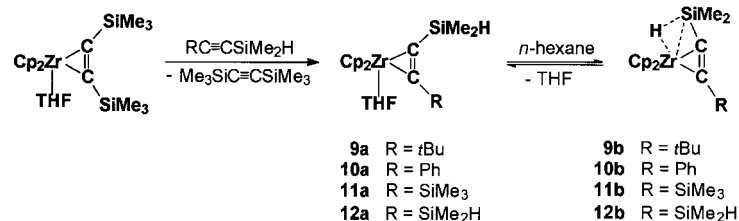
Results and Discussion

Syntheses of metallocene alkynylsilane complexes: The titanocene alkyne complexes $[\text{L}_2\text{Ti}(\text{RC}_2\text{SiMe}_2\text{H})]$ ($\text{L} = \text{Cp}$ ($\eta^5\text{-C}_5\text{H}_5$), Cp^* ($\eta^5\text{-C}_5\text{Me}_5$), THI ($\eta^5\text{-tetrahydroindenyl}$), $\text{L}_2 = \text{Me}_2\text{Si}(\eta^5\text{-C}_5\text{H}_4)_2$) can be prepared by an acetylene exchange reaction starting from the corresponding $[\text{L}_2\text{Ti}(\eta^2\text{-Me}_3\text{-SiC}_2\text{-SiMe}_3)]$ and the alkynylsilane $\text{RC}\equiv\text{CSiMe}_2\text{H}$. Since the isolation of the product from the remaining starting materials is sometimes difficult, better yields can often be obtained starting from the titanocene dichloride $[\text{L}_2\text{TiCl}_2]$. The reduction of $[\text{L}_2\text{TiCl}_2]$ with equimolar amounts of magnesium in THF in the presence of the alkynylsilanes provides their complexes in high purity and yields (Scheme 2).

The comparable zirconocene alkyne complexes with additional ligands $[\text{Cp}_2\text{Zr}(\text{thf})(\eta^2\text{-RC}_2\text{SiMe}_2\text{H})]$; $\text{R} = t\text{Bu}$ (**9a**), **Ph** (**10a**), SiMe_3 (**11a**) and SiMe_2H (**12a**) were prepared by an acetylene exchange reaction starting from $[\text{Cp}_2\text{Zr}(\text{thf})(\eta^2\text{-Me}_3\text{-SiC}_2\text{SiMe}_3)]$ and the corresponding alkynylsilanes $\text{RC}\equiv\text{CSiMe}_2\text{H}$ (Scheme 3). Upon dissolving in noncoordinating solvents, such as *n*-hexane, these complexes eliminate THF to yield zirconocene alkynylsilane complexes without additional ligands $[\text{Cp}_2\text{Zr}(\text{RC}_2\text{SiMe}_2\text{H})]$; $\text{R} = t\text{Bu}$ (**9b**), **Ph** (**10b**), SiMe_3 (**11b**) and SiMe_2H (**12b**) (Scheme 3).



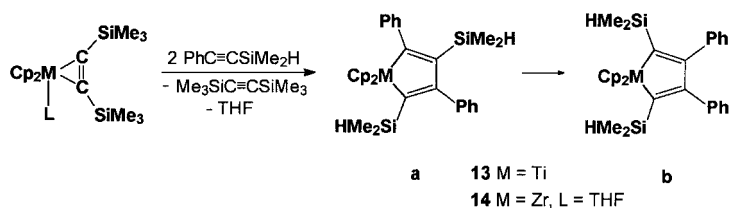
Scheme 2. Synthesis of titanocene alkyne complexes.



Scheme 3. Synthesis of zirconocene alkyne complexes.

The distinguishing characteristic feature of the metallocene alkynylsilane complexes is an interaction of the Si–H bond with the metal center, though this is strongly dependent on the electronic and steric influences of ligands and substituents. There is no agostic interaction in the case of the bulky pentamethylcyclopentadiene and tetrahydroindenyl ligands because of steric restrictions around the metal center. Similarly, the zirconium complexes containing additional donors, such as THF, exhibit no Si–H–Zr interaction. The electronic structure of the complexes, especially the electron density at the metal, is also important and plays a key role in enabling the electron donation by the Si–H bond toward the metal center.

Coupling reactions: Reactions of Group 4 metallocenes with acetylene derivatives usually result in a coupling of two acetylene molecules and the formation of a metallacyclopentadiene complex. However, this reaction depends on the three-dimensional features of the alkyne substituents; sterically demanding groups, such as R = *t*Bu or SiMe₃, prevent the coupling. In reactions of the alkynylsilanes a coupling of two acetylenes to give titana- **13a, b** and zirconacyclopentadienes **14a, b** was observed only with PhC≡CSiMe₂H. The coupling reaction is kinetically controlled and initially the unsymmetrically substituted compounds **13a, 14a** are formed preferably. A subsequent cycloreversion of the acetylene units results in the thermodynamically more stable symmetric products **13b** and **14b** (Scheme 4); the reversion proceeds slower for the titanocene cycle.

Scheme 4. The coupling reaction of the alkynylsilane PhC≡CSiMe₂H to give the titana- **13a, b** or zirconacyclopentadienes **14a, b**. Distribution of **14a:14b** after 1 h = 1:1, after 12 h = 1:3, and after 36 h = 1:10.

NMR spectroscopic measurements of the cyclic metallocenes reveal conventional Si–H resonances between $\delta = 3$ and 4, and the ²⁹Si NMR signals appear in the high-field region expected for such silanes (between $\delta = -20$ and -40). Hence the metallacyclopentadienyl complexes are metal(IV) compounds, and due to a lack of electron density there are no interactions between the d⁰-metal centers and the Si–H bonds.

IR spectroscopy: The agostic interaction of the silicon–hydrogen bond of the alkynylsilane with the metal center leads to characteristic spectroscopic properties for these complexes. This interaction is evident from IR spectra, since it causes a significant shift of the Si–H bond vibration of about 400–500 cm⁻¹ towards lower wavenumbers due to the decrease of the bond strength. This represents a considerable change of the character of the Si–H bond, as shifts, for example, for agostic Si–H–Zr

interactions were found at about 1900 cm⁻¹.^[17] Unfortunately, it is often not possible to distinguish between the stretching frequencies of the C–C triple bond and the Si–H bond, and between the complexed C–C bond and the weakened Si–H bond as they appear in the same regions. Table 1 lists the stretching frequencies $\nu(\text{Si–H})$ of the complexes compared to those of the free alkynylsilanes.

The IR data of the alkynylsilane complexes do not reveal a significant difference between the titanium and zirconium compounds with regard to the shifts of the Si–H signals upon complexation, and both metals show about the same kind of Si–H–M interaction. The only significant differences occur between complexes with and without Si–H–M interactions, as for instance **1** and **5** or between the zirconium derivatives of type **a** and **b**.

NMR spectroscopy: Typical features of the NMR spectra are a strong high-field shift of the silyl proton and a drastic decrease in the coupling constant ¹J(H,Si) (Table 1). These parameters indicate the presence of a strong Si–H–M interaction, which may be described as a three-center, two-electron bond (agostic interaction). High-field shifts are generally found for protons in bridging positions, while terminal protons in Group 4 d⁰ complexes appear at low field (e.g. [Cp₂*MH(OMe)]: M = Ti: $\delta = 3.33$,^[18] M = Zr: $\delta = 5.70$;^[19] [Cp₂ZrH(N*t*BuSiMe₂H)] $\delta = 5.53$;^[17] [(*t*Bu₃SiNH)₃ZrH] $\delta = 9.60$ ^[20]). This interpretation is supported by the hydrogen–silicon coupling constants, which are found in a range between values characteristic for one-bond interactions (¹J, 170–200 Hz) and true two-bond interactions (²J, <20 Hz), namely 68–123 Hz. A detailed interpretation of such intermediate values was given by Schubert^[11] who described complexes with strong Si–H–M interactions as frozen intermediates in the oxidative addition of Si–H to L_nM. Coupling constants of similar size were recently reported for Si–H complexes of Zr^[17] and Ru.^[21]

Some other NMR parameters are useful for describing the bonding in these complexes. The coupling

Table 1. Selected spectroscopic data (IR, NMR) of alkynylsilane complexes carrying one Si–H functionality.

Compound	No	IR $\tilde{\nu}(\text{SiH}), (\text{C}\equiv\text{C})$ [cm^{-1}]	T [K]	NMR SiMe ₂ H		¹ J(Si,H) [Hz]
				$\delta(^1\text{H})$	$\delta(^{29}\text{Si})$	
[Cp ₂ Ti(<i>t</i> BuC ₂ SiMe ₂ H)]	1	1747, 1685	303 ^[a] 193 ^[a]	– 3.74 – 7.32	– 0.5 17.6	123 93
[Cp ₂ Ti(PhC ₂ SiMe ₂ H)]	2	1752, 1737	303 ^[b]	– 5.96	21.0	99
[Cp ₂ Ti(Me ₃ SiC ₂ SiMe ₂ H)]	3	1766, 1685	297 ^[c]	– 5.24	15.4	117
[Cp ₂ [*] Ti(<i>t</i> BuC ₂ SiMe ₂ H)]	5	2081, 1614	297 ^[c]	4.47	– 36.4	183
[(THI)Ti(<i>t</i> BuC ₂ SiMe ₂ H)]	7	2090	297 ^[c]	3.97	– 35.4	185
[Me ₂ Si(η^2 -C ₃ H ₄) ₂ Ti(<i>t</i> BuC ₂ SiMe ₂ H)]	8	1753	299 ^[a] 224 ^[a]	– 6.54 – 7.24	7.4 11.4	100 94
[Cp ₂ Zr(thf)(<i>t</i> BuC ₂ SiMe ₂ H)]	9a	2094, 1688	217 ^[b]	4.58	– 26.5	174
[Cp ₂ Zr(thf)(PhC ₂ SiMe ₂ H)]	10a	2064, 1683	213 ^[b]	4.37	– 22.2	175
[Cp ₂ Zr(thf)(Me ₃ SiC ₂ SiMe ₂ H)]	11a	2086, 1699	246 ^[b]	4.54	– 23.6	179
[Cp ₂ Zr(<i>t</i> BuC ₂ SiMe ₂ H)]	9b	1689	297 ^[c] 217 ^[b]	– 3.74 – 3.69	16.1 18.2	72 72
[Cp ₂ Zr(PhC ₂ SiMe ₂ H)]	10b	1688, 1617	233 ^[a]	– 3.55	20.6	88 ^[e]
[Cp ₂ Zr(Me ₃ SiC ₂ SiMe ₂ H)]	11b	1700 (br)	297 ^[c] 229 ^[b]	– 4.29 – 4.27	34.3 35.7	68 68
<i>free alkynylsilanes</i>						
<i>t</i> BuC≡CSiMe ₂ H		2139, 2157	303 ^[e]	4.31	– 38.6	200
PhC≡CSiMe ₂ H		2141, 2161	303 ^[e]	4.31	– 37.3	202
Me ₃ SiC≡CSiMe ₂ H		2114, 2144	303 ^[d]	4.37	– 38.9	201
HMe ₂ SiC≡CSiMe ₂ H		2094, 2145	303 ^[d]	4.12	– 38.6	202

[a] [D₈]toluene. [b] [D₈]THF. [c] C₆D₆. [d] CDCl₃. [e] 303 K.

constant ³J(SiH,CH₃) is 3.8 Hz for the free silanes and decreases or even vanishes in the alkynylsilane complexes because of the reduction of the Si–H bond order. Consequently, the Si–C bond order increases (towards a double bond), and the ²⁹Si NMR signal is shifted more than 50 ppm downfield to a region where the resonances of sp² hybridized silicon atoms, such as in silenes or sila-allenes ($\delta > 10$), are expected.^[22] However, the trend for the ²⁹Si NMR shift upon Si–H activation is not a general one, downfield shifts (at Mn^[23]) were found as well as strong upfield shifts (at Ru^[21] or Zr^[17]).

Another two parameters are specific for the bonding in the alkynylsilane complexes: the shifts of the cyclopentadienyl ligand and the quaternary Si-substituted carbon atom. Titanocene alkyne complexes are best described as metallacycloprenes (Ti^{IV} or d⁰ compounds);^[24] their cyclopentadienyl NMR signals appear at low field (cf. [Cp₂Ti(η^2 -*t*BuC₂SiMe₃)] $\delta_{\text{H}} = 6.5$, $\delta_{\text{C}} = 117$ ^[25]). However, for the titanocene (and zirconocene) alkynylsilane complexes we find these signals at remarkably higher field (complex **1**: $\delta_{\text{H}}(193 \text{ K}) = 4.8$, $\delta_{\text{C}}(193 \text{ K}) = 101$). The Si–H–M interaction emulates coordination of a further ligand and changes the electron density at the metal center; according to ab initio calculations,^[15] complex **1** is best described as a d² compound. The shift of the quaternary Si-substituted carbon atom is completely unlike that of an alkyne complex (cf. [Cp₂Ti(η^2 -*t*BuC₂SiMe₃)]: $\delta = 205$;^[25] complex **1**: $\delta = 89.4$ (193 K)). This shift is difficult to rationalize, but an important contribution might be made by the unusual coordination geometry around this quaternary carbon atom. The bond angle Si–C–C is only 150°,^[14] and it is possible to define a plane through the carbon in such a way that all atomic neighbors reside on the same side of this plane. In other words, the side opposite the titanium is completely naked. A similar situation is found in 1,3-butadiyne complexes that may

also be regarded as metallacyclocumulenes (Figure 1), where the β -carbon atoms give NMR signals at $\delta = 95$ (M = Ti, R = *t*Bu^[26]) or $\delta = 106$ (M = Zr, R = *t*Bu^[27]).

These shifts, however, indicate a fundamental difference between complexes of alkynylsilanes and complexes of other alkynes. Compounds lacking the strong Si–H–M interaction (**5–7**, **9a–12a**) are characterized by parameters similar to those applied to common alkyne complexes,^[28] and the data for the SiMe₂H group differ little from those of the free silanes.

Dynamic behavior and temperature dependence in solution:

The chemical shifts and coupling constants of most of the complexes are found to be strongly temperature dependent (Table 1). At low temperature the spectra exhibit the features indicative of strong Si–H–M interactions. When the sample is heated, all these parameters change and become more appropriate for a species without an activated Si–H bond (the proton signal moves downfield). However, no line broadening or any second species is observed over the accessible temperature range for the complexes with only one Si–H function.

Complex **4**, which contains two Si–H functions, shows an additional effect. Only one of the Si–H bonds is activated, the other one remains unaffected. The NMR signals of the two different S–H bonds are observed separately at low temperature (Table 2), but upon heating they broaden, merge, and eventually show up as an averaged signal, but not in the middle where it is expected. Instead, the averaged signal is shifted downfield, and this shift increases with temperature, as found for the monofunctional complexes. The first of these two phenomena, connected with line broadening, can be

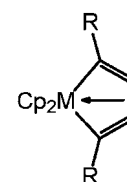


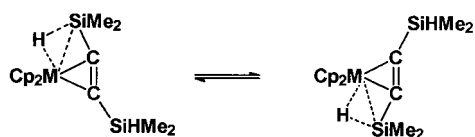
Figure 1. Structural formula of metallacyclocumulenes.

Table 2. Selected NMR data for complexes carrying two Si–H functions.

Compound [M](HMe ₂ SiC ₂ SiMe ₂ H)	Temperature [K]	¹ H NMR			²⁹ Si NMR		
		free	SiMe ₂ H	Cp	SiMe ₂ H free	(¹ J _{SiH} [Hz]) coord	
4 [M] = Cp ₂ Ti	356 ^[a]		0.41			–9.6 (161)	
	303 ^[b]		–0.39			–3.0 (152)	
	165 ^[b]	4.58		–8.04	4.94	–22.8 (186) –33.4 (184)	34.3 (92)
6 [M] = Cp ₂ [*] Ti	303 ^[c]	4.49		–		–	
12a [M] = Cp ₂ Zr(thf)	300 ^[d]	4.71		–	5.25	–	
	246 ^[d]	4.58		–	5.57	–	
	203 ^[d]	4.44		–	5.58	–21.3 (176) –28.0 (178)	–
		4.74					
12b [M] = Cp ₂ Zr	365 ^[a]		0.50		4.93		
	290 ^[a]	4.98		–4.35	4.93	–21.8 (190) –21.6 (187)	34.8 (70)
	246 ^[a]	5.05		–4.40	4.93		35.3 (69)

[a] [D₈]toluene. [b] (C₂D₅)₂O. [c] C₆D₆. [d] [D₈]THF.

easily explained by an alternating interaction of the Si–H groups with the titanium center (flip-flop coordination, Scheme 5).



Scheme 5. The alternating interaction (flip-flop coordination) of the Si–H groups about the metal center.

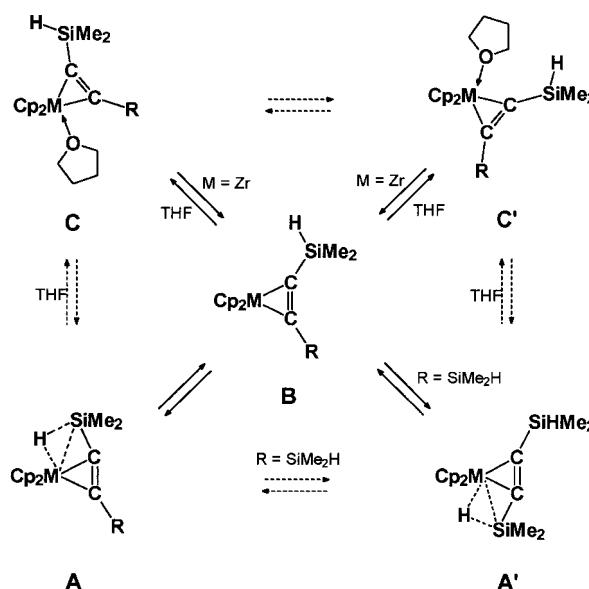
The explanation of the second phenomenon, the extraordinary temperature-dependent shifts and coupling constants, is less apparent. One could assume that the strength of the Si–H–Ti interaction is determined by temperature (a single-minimum potential, which could be defined in a simplified way, in that the preferred position of the H atom is closer to the metal upon cooling and closer to silicon upon heating). Such a process would only require minimal rearrangements of the atomic skeleton and should possibly occur also in the crystal. The chemical shifts for complex **1** in the solid state at ambient temperature (Table 3) are close to those observed in solution at very low temperature, where further cooling has almost no more effect and the signals do not show strong temperature shifts. The values in Table 3 should therefore also be appropriate for the structure of **1** determined by X-ray crystallography. As the values are almost independent of temperature, this experiment makes the model described above (single-minimum potential) less probable.

Another possible explanation would be the existence of a very fast equilibrium between the species with an activated

Table 3. Comparison of NMR data of **1** in solution and solid-state.

		291 K solid	320 K solid	193 K [D ₈]toluene	303 K [D ₈]toluene	356 K [D ₈]toluene
δ(¹³ C)	Cp	102.1, 101.8	102.2, 101.9	100.8	105.8	109.8
	CMe ₃	40.0	40.0	39.3	40.6	41.6
	CMe ₂	34.2	34.2	32.9	32.6	32.3
	SiMe ₂	–1.1, –1.7	–1.0, –1.6	–3.0	–2.5	–2.2
	C(<i>t</i> Bu)	207.8	207.9	206.1	216.2	224.5
	C(Si)	92.5	92.9	89.4	116.4	
δ(²⁹ Si)	SiMe ₂ H	16.7	16.1	17.6	–0.5	

Si–H bond and a common alkyne complex (a double-minimum potential, represented by **A** and **B**, Scheme 6). At low temperature, **A** would be the preferred species. At higher temperature, the population of **B** should increase (for entropic reasons, because the molecule gains another degree



Scheme 6. Dynamic behavior of the zirconocene and titanocene complexes, which may explain the behavior of the averaged Si–H NMR signal at different temperatures.

of freedom: the rotation about the Si–C bond), and the NMR parameters (which are always averaged values) suggest a less activated species. Because of the limited thermal stability of the titanium complexes it was not possible to drive the equilibrium completely to the side of **B**, and even at the highest accessible temperatures (330–350 K), the influence of a Si–H–Ti interaction is clearly visible.

For the zirconium complexes **9–12** the situation is even more complicated. The solvent-free species behave similar to the respective titanium complexes, but the temperature dependence is not as great. The intermediate **B** seems to be energetically less favored for Zr than for Ti, and this is not surprising since it is known that zirconocene alkyne complexes have a

greater tendency to coordinate additional ligands than the corresponding titanocene alkyne complexes.^[29] Recently equilibria have been studied between solvent-free complexes $[L_2Zr(\text{alkyne})]$ and the solvates $[L_2Zr(\text{thf})(\text{alkyne})]$, $L = \text{cyclopentadienyl derivative}$.^[30] If the zirconium complexes **9–12** are dissolved in THF, the solvent competes successfully with the Si–H bond at the metal center (Scheme 6, **A** and **C**). At low temperatures, THF coordination is favored (complex **12a:12b** = 14:1 at 203 K), but at higher temperatures, dissociation of the solvate is preferred, again for entropic reasons, and the Si–H function occupies the free coordination site (complex **12a:12b** = 1:1.3 at 290 K).

The discussed species could be identified in cold solutions of **10** and **12** in THF (Table 3), and their interconversion has been proven by magnetization transfer experiments in the region of slow exchange. At 203 K, there are four distinguishable Si–H groups for **12**, two for the degenerate rotational isomers of **12a** (**C** and **C'**, $R = \text{SiMe}_2\text{H}$), and two for **12b**, for which the flip-flop between **A** and **A'** is frozen out. On heating the sample, the signals of **12a** coalesce first (because of an exchange between **C** and **C'** by alkyne rotation or interchange of the solvent ligand; this behavior is known for such alkyne complexes^[31]). A broadening of the **A** and **A'** resonances occurs then, and finally all signals merge and only one set of signals, representing the average of all four species, is observed above room temperature. Complex **10** exhibits three Si–H groups at 213 K, two for the rotational isomers **C** and **C'** of **10a**, which are no longer degenerate ($R = \text{Ph}$), and the third for the activated function of **10b** (**A** in Scheme 6).

The existence of the intermediate **B** is not an absolute necessity to understand the dynamic behavior of the zirconocene complexes (dotted arrows in Scheme 6). Its postulated existence allows, however, a straightforward explanation of the described temperature-dependent NMR parameters, particularly for the titanocene complexes. A final decision on the relevance (and the exact bonding) of **B** cannot be made because in no case were values (for example, chemical shifts of the silyl proton; Table 1) found that resemble those of the titanocene or zirconocene species in which a Si–H–M interaction is definitely excluded (for example, **5** or **11a**).

Fan and Lin^[15] calculated the stabilization of the titanium complex **1** by the strong Si–H–Ti interaction to be about 33 kJ mol^{-1} . An estimation of the activation barrier for the flip-flop process for the titanium complex **4** (from the coalescence of signals for the Si–H or Me groups) gives a value of ΔG_{190}^\ddagger of 37 kJ mol^{-1} . If we assume an equilibrium between **A**, **B** and **A'** (Scheme 6), we may take the chemical shift of the averaged Si–H signal as representing the equilibrium constant between **A** and **B**. From its temperature dependence, a reaction enthalpy ΔH of about -18 kJ mol^{-1} for the process **B** \rightarrow **A** in hexane can be derived. These are very rough estimates (because of the limited number of data points and the uncertainties in the determination of T), but as the values are all of the same magnitude they are consistent with the assumption that the discussed equilibria are not unreasonable.

For complex **12b**, the zirconium analogue of **4**, a free activation enthalpy ΔG_{350}^\ddagger of 60 kJ mol^{-1} (in toluene) was estimated for the flip-flop process. This is consistent with the

assumption that the Si–H–M interaction in the zirconocene complexes is somewhat stronger than in the titanocene analogues.

Crystallographic characterization: In addition to the already crystallographically characterized titanium complex **1**,^[14] we obtained suitable single crystals of the solvent-free zirconium complex **12b** (Table 4). The structure determined (Figure 2) enabled the two metallocenes with different central metals to be compared with regard to the silicon-hydrogen-metal interaction, because the interacting hydrogen atom could be found and refined.

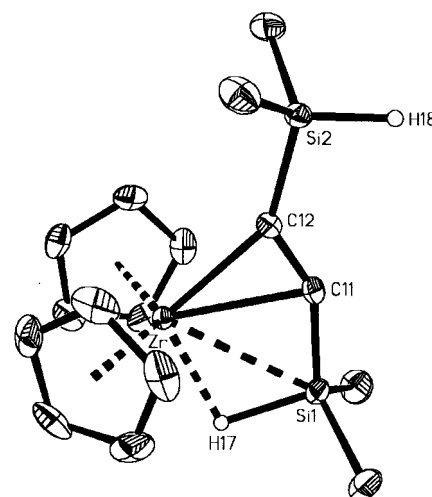


Figure 2. Perspective view (ORTEP) of complex **12b**.

Table 4. Crystal data and structure refinement for **12b**.

empirical formula	$\text{C}_{16}\text{H}_{24}\text{Si}_2\text{Zr}$
formula weight	363.75
crystal system	monoclinic
space group	$P2_1/n$
unit cell dimensions	
a [Å]	8.661(2)
b [Å]	13.927(3)
c [Å]	14.754(3)
β [°]	99.62(3)
volume	$1754.6(7) \text{ \AA}^3$
Z	4
ρ_{calc}	1.377 g cm^{-3}
absorption coefficient	0.750 mm^{-1}
$F(000)$	752
crystal color	red
crystal description	prism
crystal size	$0.5 \times 0.4 \times 0.4 \text{ mm}$
temperature [K]	200(2)
radiation	$\text{MoK}\alpha$
measurement device	Stoe-IPDS
theta range for data collection	2.02 to 24.23°
index ranges	$-9 \leq h \leq 9$, $-15 \leq k \leq 16$, $0 \leq l \leq 16$
independent reflections	2663 [$R(\text{int}) = 0.030$]
reflections observed [$I \geq 2\sigma(I)$]	2475
data/restraints/parameters	2663/0/174
R indices [$I \geq 2\sigma(I)$]	$R_1 = 0.026$, $wR_2 = 0.067$
R indices (all data)	$R_1 = 0.029$, $wR_2 = 0.081$
goodness of fit on F^2 (all data)	1.191
largest difference peak and hole	0.46 and -0.46 e \AA^{-3}

Complexes of alkynylsilanes containing an Si-H-metal interaction display a *trans* configuration of the alkyne ligand in contrast to the common *cis* arrangement.^[29] The previously discussed significant reduction of the silicon-hydrogen bond order due to the presence of a Si-H-M interaction, which had already been supported by NMR spectroscopic (coupling constant $^1J_{\text{SiH}}$) data, is confirmed by the X-ray crystallographic data (Table 5). Almost identical structures were found for

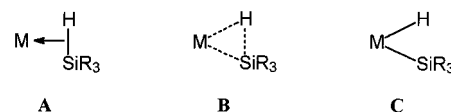
Table 5. Selected bond lengths and angles of the zirconocene complex **12b** (M = Zr, R = SiMe₂H) in comparison to the corresponding data of the titanocene **1** (M = Ti, R = *t*Bu).

[Cp ₂ M(R-C12=C11-Si1HMe ₂)]	12b	1
distances [Å]		
M-Si1	2.758(1)	2.655(2)
M-H	2.042(4)	1.82(5)
M-C11	2.407(3)	2.276(7)
M-C12	2.299(3)	2.162(7)
C11-C12	1.291(4)	1.275(9)
C11-Si1	1.787(3)	1.766(6)
Si1-H17	1.634(4)	1.42(6)
angles [°]		
C11-Si1-H17	106.7(2)	98(2)
Si1-C11-C12	150.2(2)	149.5(6)
R-C12-C11	134.1(2)	135.2(7)

both compounds with only small differences attributed to different covalent radii of the central atoms. The most important feature of the alkynylsilanes are the relative positions of the metal, Si, and H atoms. The metal-hydrogen (**12**: Zr-H 2.042(4); **1**: Ti-H 1.82(5) Å) and metal-silicon (**12**: Zr-Si 2.758(1); **1**: Ti-Si 2.655(2) Å) distances are rather short and fall within the range of normal single bond lengths observed for a variety of metalocene complexes containing M-H or M-Si bonds.^[32] The M-H distances are remarkably short and similar to those observed in metalocene hydrides. Surprisingly, the Si-H bonds also do not show significant lengthening (Si-H: 1.634(4) Å for **12b**, 1.42(6) Å for **1**) and fall within the region expected for tetrahedral silanes.^[11a] However, the distinct difference of 0.2 Å between both Si-H distance confirms a strong steric influence around the central atom and suggests that the relative small space between silicon and hydrogen is forced by a three-dimensional congestion in the neighborhood of the metal. Another important structural characteristic of both complexes is the shortened Si-C distances of 1.766(6) Å (**1**) and 1.787(3) Å (**12b**), which reveals a certain double-bond character.^[33] Together with a stronger metal coordination (M-C distances, Table 5) of C12 than of C11, these data would be expected in the case of a complete hydrogen transfer to the metal and the formation of silaallene structure (see Scheme 7, Structure **B**) which would contradict the observation of a silicon-hydrogen coupling constant in the NMR spectra.

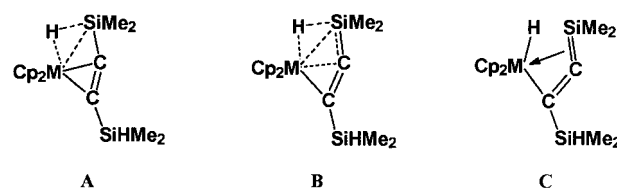
Characterization of the Si-H-M interaction in alkynylsilane metalocene complexes: In general, silicon-hydrogen bonds are particularly good electron donors toward transition metals. These interactions have been studied in detail and

some Group 4 metallocenes containing such interactions have already been isolated.^[11, 17, 32, 34] Usually, Si-H-M interactions can be described by the three different structures **A**, **B**, and **C** (Scheme 7). Structure **A** can be considered as one in which a



Scheme 7. Three different ways to describe the Si-H-M interaction.

sole σ -donation of the Si-H bond towards an unoccupied d orbital of the metal occurs. Structure **B** is characterized by an additional π -type interaction between a filled metal d orbital and the σ^* orbital of the Si-H bond. The Si-H bond order is reduced by both interactions and an even stronger activation can lead to an oxidative addition with a complete Si-H bond cleavage (structure **C**). Since the three-center, two-electron interaction in the described alkynylsilane complexes seems to gradually intensify upon decreasing temperature it was necessary to consider whether the strengthening of the bond can result in a complete oxidative addition of the Si-H bond at the metal with the formation of a metal hydride silaallenyl structure (Scheme 8, Structure **C**).



Scheme 8. Three different resonance structures to describe the Si-H-M interaction in alkynylsilane metalocene complexes. The structure **C** becomes more important as the temperature is lowered.

In the case of the described Group 4 metallocene complexes with alkynylsilane derivatives carrying Si-H functionalities we can not unambiguously prove a complete oxidative addition of the Si-H bonds to the metal centers, even though some spectroscopic data suggest a considerable importance of the resonance structure **C**, particularly at low temperatures and in the solid state. The most striking indications supporting a silaallenyl hydride structure are certainly the ²⁹Si NMR resonances, which lie above $\delta = 20$ in the specific region of sp²-hybridized silicon atoms, and the huge difference in the chemical ¹³C NMR shifts of the acetylenic carbon atoms. The carbon atoms carrying the Si-H group appear remarkably upfield at around $\delta = 115$, whereas the other C signal is found above $\delta = 200$, typical for metal-bonded sp² carbon atoms. The difference increases at lower temperatures with high-field shifts of the allenyl carbon up to 90 ppm (see data of **1**, Table 3). Similar differences were observed for cyclic cumulenes with central bent allenyl atoms (difference about 105 ppm; see discussion above). The cyclic cumulene structure of these complexes^[26, 27] was unprecedented and highly unexpected due to the strain of the cycle. Meanwhile this structure has been calculated to be thermodynamically very stable and its existence has been proved by theoretical methods.^[35] Further

indications of a silaallenyl hydride come from X-ray diffraction analyses. Besides short M–H and M–Si bond lengths normally associated with common single bonds, the crystal structures of **1**^[14] and **12b** show a significant shortening of the Si–C distances towards Si=C double bonds consistent with a coordinatively stabilized silaallenyl structure, resulting from steric crowding which forces the hydride close to the silicon.

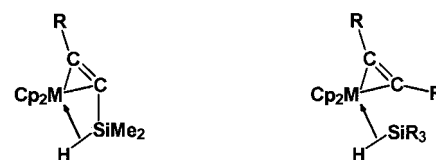
On the other hand the mesomeric structure **A** (Scheme 8) is supported by the fact that the Si–H distances of both complexes (**1** and **12b**) are not too great in the crystal and fall within the range of silicon–hydrogen bonds. Also the remarkable Si–H coupling constant of about 70–90 Hz is a sign of a silicon–hydrogen interaction, even though the homonuclear coupling $^3J_{\text{H,H}}$ between the Si–H and the Si-methyl protons is drastically reduced at low temperatures. One could argue whether the Si–H coupling is a one-bond coupling or whether it is more appropriate to attribute it to a two-bond coupling $^2J_{\text{Si,H}}$. Examples for such 2J couplings are known and range from less than 10 Hz up to 70 Hz,^[32a] although the question has been asked whether the high values represent genuine two-bond interactions or whether they contain contributions from direct bonding.^[23] Three-dimensional crowding around the central metal could also be a reason for the lack of a complete separation of Si and H, as the hydride is forced close to the silicon by steric hindrance. A puzzling result, which can be considered as untypical for Group 4 metallocene hydrides, is the extreme upfield shift of the hydrogen signal, as common hydrides are usually shifted downfield (see discussion above).

Conclusions

In conclusion, a supposed hydrogen transfer at low temperatures cannot be ruled out but requires further investigations of the reaction behavior of alkynylsilane complexes. Judged by the spectroscopic IR and NMR data the structure of the silane complexes is best described as an agostic three-center, two-electron interaction between the Si–H bond and the metal center (Scheme 8, **B**). A considerable strengthening of this interaction is observed in solution upon decreasing the temperature. This continues until a certain limit is reached and the agostic interaction becomes frozen at a state close to the hydridosilyl extreme. One could speak of an arrested hydrogen transfer along the reaction coordinate, which represents the oxidative addition of the Si–H bond at the metal.

Relationship to catalytic reactions: The titanocene and zirconocene complexes with *intramolecularly* coordinating alkynylsilanes can serve as suitable model compounds to study the *intermolecular* interaction of similar alkyne complexes with silanes, which are used in catalytic reactions such as the hydrosilylation of aldimines and ketimines^[36] and the dehydrogenative polymerization of silanes^[37] (Scheme 9).

The assumed first step in the catalytic reactions is the interaction with the silane. Whether these interactions are possible or not is strongly dependent on the ligands L (Cp or



Scheme 9. The titanocene and zirconocene complexes with intramolecularly coordinating alkynylsilanes (left) are potential models to study the intermolecular interaction of similar complexes (right), which are used in catalytic reactions.

Cp*), the size of the metals (Ti or Zr), and the substituents of the alkyne R (Ph or SiMe₃) in the complexes [$L_2M(\eta^2\text{-RC}_2\text{R})$]. In this respect, there are some similarities to the coordination of a second ligand L' to obtain complexes of the type [$L_2M(L')(\eta^2\text{-RC}_2\text{R})$]. Here the size of L' in combination with the size of M makes such complexes stable or not.^[30]

In the above-mentioned catalytic systems we used silanes that differed in size (PhMe₂SiH, Ph₂SiH₂, and PhSiH₃), but in our alkynylsilane complexes this effect is not considered because all complexes contain a silane R–C≡CSiMe₂H. This allowed us to study the influences of L and M.

In a series of investigated precatalysts for the dehydrogenative polymerization of hydrosilanes, the complexes [$L_2M(\eta^2\text{-Me}_3\text{SiC}_2\text{SiMe}_3)$] with L = Cp are the most active (compared to other ligands L such as Cp*). This is surprising, because Tilley described the formation of catalytically inactive hydride-bridged dimers starting from [Cp_2Zr] complexes, but found a slow dehydrocoupling by using [Cp_2^*Zr] complexes.^[7] The result of our comparison is that those combinations of L and M that allow an intensive interaction of the alkynylsilane with the metal are also the best suited precatalysts, in agreement with the above-mentioned data.

Experimental Section

General data: All manipulations were carried out under an inert atmosphere of argon by using standard Schlenk techniques. Solvents were freshly distilled from sodium tetraethylaluminate prior to use. NMR spectra were recorded on a Bruker ARX 400 (solution) or MSL 300 (solid state) spectrometer. Chemical shifts are given on the δ scale relative to SiMe₄ and were referenced against the solvent signals. Solid-state spectra were recorded by the CP/MAS technique (ZrO₂ rotors, 4 mm o.d.) and referenced against external adamantane ($\delta(^{13}\text{C}) = 38.4$) or Q₈M₈ siloxane^[38] ($\delta(^{29}\text{Si}) = 11.6$). IR data were obtained on a Nicolet Magna 500 (Nujol mulls using KBr plates). X-ray crystallographic data were collected with a STOE-IPDS diffractometer using graphite-monochromated MoK α radiation. The structure was solved by direct methods (SHELXS-86)^[39] and refined by full-matrix least-squares techniques against F^2 (SHELXL-93).^[40]

Preparation of alkynylsilane complexes: a) A solution of the alkynylsilane RC≡CSiMe₂H (1 mmol; R = *t*Bu, Ph, SiMe₃, SiMe₂H) in THF (15 mL) was added to a mixture of magnesium turnings (1.1 mmol) and the appropriate metallocene dichloride [$L_2\text{MCl}_2$] (1 mmol; M = Ti, Zr; L = Cp ($\eta^5\text{-C}_5\text{H}_5$), Cp* ($\eta^5\text{-C}_5\text{Me}_5$), THI ($\eta^5\text{-tetrahydroindenyl}$); L₂ = Me₂Si($\eta^5\text{-C}_5\text{H}_4$)₂). After the reduction was complete (about 4 h at ambient temperature) the solvent was removed in vacuo and replaced by *n*-hexane (15 mL). Filtration and subsequent evaporation to dryness led to the alkynylsilane complex, which could be recrystallized from a solution in *n*-hexane at –30 °C. b) Starting from the bis(trimethylsilyl)acetylene complexes [$L_2M(L)(\eta^2\text{-Me}_3\text{SiC}_2\text{SiMe}_3)$] in THF the acetylene ligand can be substituted by an equimolar amount of an alkynylsilane because of the higher stability of Si–H complexes. After evaporation of THF *n*-hexane was added and the solution filtered. To obtain the pure alkynylsilane complexes the products had to be

separated from the starting metallocene by crystallization at lower temperatures. This reduced the yields by about 15–25%. Separated products were washed with cold hexane and dried in vacuo.

Preparation of metallacyclopentadiene complexes: The alkynylsilane $\text{PhC}_2\text{SiMe}_2\text{H}$ (0.32 g, 2.0 mmol) was added to a solution of the bis(trimethylsilyl)acetylene complexes $[\text{L}_2\text{M}(\text{L})(\eta^2\text{-Me}_3\text{SiC}_2\text{SiMe}_3)]$ (1.0 mmol) in *n*-hexane (15 mL). After the reduction was complete (about 4 h at 40 °C) the solvent was removed in vacuo and replaced by a *n*-hexane/THF mixture (3/1, 20 mL). Filtration and subsequent crystallization led to the metallacyclopentadiene complex. Separated products were washed with cold hexane and dried in vacuo.

[Cp₂Ti(*t*BuC₂SiMe₂H)] (1): [Compound **1** has already been spectroscopically characterized.]^[14] Yield: Method a) 67%, method b) 46%, dark red crystals. ¹H NMR ([D₈]toluene, 303 K): $\delta = -3.74$ (sept, 1H; SiH), -0.02 (d, ³J(H,H) = 2.5 Hz, 6H; SiMe₂), 1.05 (s, 9H; *t*Bu), 5.28 (s, 10H; Cp); ¹³C NMR ([D₈]toluene, 303 K): $\delta = -2.5$ (¹J(Si,C) = 61 Hz; SiMe₂), 32.6 (CMe₃), 40.6 (CMe₃), 105.8 (Cp), 116.4 (CSiMe₂), 216.2 (CCMe₃); ²⁹Si NMR ([D₈]toluene, 303 K): $\delta = -0.5$ (¹J(Si, H) = 123 Hz). IR (Nujol): $\tilde{\nu} = 1685, 1747 \text{ cm}^{-1}$ (SiH, C≡C_{coord}). C₁₈H₂₆SiTi (318.4): calcd: C 67.91, H 8.23; found: C 67.57, H 8.11.

[Cp₂Ti(PhC₂SiMe₂H)] (2): Yield: Method a) 42%, violet crystals, m.p. 125–130 °C. ¹H NMR ([D₈]THF, 303 K): $\delta = -5.96$ (sept, 1H; SiH), 0.46 (d, ³J(H,H) = 2.0 Hz, 6H; SiMe₂), 5.15 (s, 10H; Cp), 7.22 (1H; *p*-Ph) 7.36 (2H; *m*-Ph) 7.61 (2H; *o*-Ph); ¹³C NMR ([D₈]THF, 303 K): $\delta = -2.9$ (SiMe₂), 102.9 (Cp), 109.6 (CSiMe₂), 128.1 (*p*-Ph), 128.7, 132.8 (CH Ph), 139.0 (*i*-Ph), 195.8 (CPh); ²⁹Si NMR ([D₈]THF, 303 K): $\delta = 21.0$ (¹J(Si, H) = 99 Hz). IR (Nujol): $\tilde{\nu} = 1737, 1752 \text{ cm}^{-1}$ (SiH, C≡C_{coord}). C₂₀H₂₂SiTi (338.4): calcd: C 71.00, H 6.55; found: C 70.64, H 6.40.

[Cp₂Ti(Me₃SiC₂SiMe₂H)] (3): Yield: Method a) 53%, violet oily solid. ¹H NMR (C₆D₆, 297 K): $\delta = -5.24$ (1H; SiH), 0.11 (d, ³J(H,H) = 2.2 Hz, 6H; SiMe₂), 0.20 (s, 9H; SiMe₃), 5.22 (s, 10H; Cp); ¹³C NMR ([D₈]toluene, 303 K): $\delta = -2.7$ (SiMe₂, SiMe₃), 103.8 (Cp), 117.7 (CSiMe₂), 202.8 (CSiMe₃); ²⁹Si NMR (C₆D₆, 297 K): $\delta = -8.5$ (SiMe₃), 15.4 (¹J(Si,H) = 117 Hz, SiMe₂). IR (Nujol): $\tilde{\nu} = 1685, 1766 \text{ cm}^{-1}$ (SiH, C≡C_{coord}). C₁₇H₂₆Si₂Ti (334.4): calcd: C 61.05, H 7.84; found: C 60.71, H 7.51.

[Cp₂Ti(HMe₂SiC₂SiMe₂H)] (4): Yield: Method b) 61%, violet crystals, m.p. 142–146 °C. ¹H NMR (C₆D₆ at 303 K: averaged data, see also Table 2): $\delta = -0.96$ (2H; SiH), 0.27 (d, ³J(H, H) = 2.9 Hz, 12H; SiMe₂), 5.02 (s, 10H; Cp); ¹³C NMR (C₆D₆, 303 K): $\delta = -2.2$ (¹J(Si, C) = 57 Hz, SiMe₂), 103.0 (Cp), 162.3 (CSiMe₂); ²⁹Si NMR (C₆D₆, 303 K): $\delta = 0.5$ (¹J(Si, H) = 147 Hz). IR (Nujol): $\tilde{\nu} = 1759, 1771 \text{ cm}^{-1}$ (SiH, C≡C_{coord}), 2106 cm⁻¹ (SiH_{free}). C₁₆H₂₄Si₂Ti (320.4): calcd: C 59.98, H 7.55; found: C 59.65, H 7.37.

[Cp₂Ti(η^2 -*t*BuC₂SiMe₂H)] (5): Yield: Method a) 51%, yellow-brown crystals, m.p. 90–92 °C. ¹H NMR (C₆D₆, 297 K): $\delta = 0.12$ (d, ³J(H, H) = 3.6 Hz, 6H; SiMe₂), 0.99 (s, 9H; *t*Bu), 1.80 (s, 30H; Cp*), 4.47 (sept, 1H; SiH); ¹³C NMR (C₆D₆, 297 K): $\delta = 1.7$ (SiMe₂), 13.0 (C₅Me₃), 33.3 (CMe₃), 43.7 (CMe₃), 122.0 (C₅Me₃), 208.7 (CSiMe₂), 242.7 (CCMe₃); ²⁹Si NMR (C₆D₆, 297 K): $\delta = -36.4$ (¹J(Si, H) = 183 Hz). IR (Nujol): $\tilde{\nu} = 2081 \text{ cm}^{-1}$ (SiH), 1614 cm⁻¹ (C≡C_{coord}). C₂₈H₄₆SiTi (458.6): calcd: C 73.33, H 10.11; found: C 73.02, H 9.87.

[Cp₂Ti(η^2 -HMe₂SiC₂SiMe₂H)] (6): Yield: Method a) 52%, yellow-green powder, m.p. 86–90 °C. ¹H NMR (C₆D₆, 303 K): $\delta = 0.52$ (d, ³J(H, H) = 3.7 Hz, 12H; SiMe₂), 1.70 (s, 30H; Cp*), 4.49 (sept, ³J(H, H) = 3.7 Hz, 2H; SiH); ¹³C NMR (C₆D₆, 303 K): $\delta = 0.1$ (SiMe₂), 12.4 (C₅Me₃), 122.0 (C₅Me₃), 245.1 (CSiMe₂); ²⁹Si NMR (C₆D₆, 303 K): $\delta = -33.4$ (¹J(Si, H) = 184 Hz). IR (Nujol): $\tilde{\nu} = 1577 \text{ cm}^{-1}$ (C≡C_{coord}), 2090 cm⁻¹ (SiH_{free}). C₂₆H₄₄Si₂Ti (460.7): calcd: C 67.79, H 9.63; found: C 67.41, H 9.95.

[(THD)₂Ti(η^2 -*t*BuC₂SiMe₂H)] (7): Yield: Method a) 66%, red-brown oil. ¹H NMR (C₆D₆, 297 K): $\delta = 0.10$ (d, ³J(H, H) = 2.5 Hz, 6H; SiMe₂), 0.74 (s, 9H, *t*Bu), 1.25 (m, 4H; CH₂), 1.40, 1.55, 1.75, 2.30, 2.45, 2.95 (m, 2 H each; CH₂), 3.97 (1H, SiH), 5.35, 5.68, 7.00 (2 H each; CH); ¹³C NMR (C₆D₆, 297 K): $\delta = 0.6$ (SiMe₂), 23.4, 23.8, 25.2, 25.7 (CH₂), 31.6 (CMe₃), 42.5 (CMe₃), 110.9, 111.1, 113.2 (CH), 125.6 (double intensity, 2 C_q), 198.7 (CSiMe₂), 237.8 (CCMe₃); ²⁹Si NMR (C₆D₆, 297 K): $\delta = -35.4$ (¹J(Si, H) = 185 Hz). IR (Nujol): $\tilde{\nu} = 2090 \text{ cm}^{-1}$ (SiH), 1653 cm⁻¹ (C≡C_{coord}). C₂₆H₃₈SiTi (426.6): calcd: C 73.21, H 8.98; found: C 73.57, H 9.24.

[(Me₂Si(η^5 -C₅H₄))₂Ti(*t*BuC₂SiMe₂H)] (8): Yield: Method a) 71%, violet oily crystals. ¹H NMR ([D₈]toluene, 299 K): $\delta = -6.54$ (1H; SiH), 0.13 (d, ³J(H, H) = 2.0 Hz, 6H, SiMe₂H), 0.18, 0.28 (s, 3 H each; SiMe₂), 1.29 (s, 9H; *t*Bu), 4.72, 5.04, 5.18, 6.08 (m, 2 H each; C₅H₄); ¹³C NMR ([D₈]toluene,

299 K): $\delta = -5.5, -5.0$ (SiMe₂), -2.2 (¹J(Si, C) = 64 Hz; SiMe₂H), 33.2 (CMe₃), 40.3 (CMe₃), 98.2 (CSiMe₂H), 98.8 (C_q), 97.9, 101.9, 108.5, 117.5 (CH), 209.0 (CCMe₃); ²⁹Si NMR ([D₈]toluene, 299 K): $\delta = -16.6$ (SiMe₂); 7.4 (¹J(Si, H) = 100 Hz; SiMe₂H). IR (capillary): $\tilde{\nu} = 1753 \text{ cm}^{-1}$ (SiH, C≡C_{coord}). C₂₀H₃₀Si₂Ti (374.5): calcd: C 64.14, H 8.07; found: C 63.83, H 8.41.

[Cp₂Zr(thf)(η^2 -*t*BuC₂SiMe₂H)] (9a): Yield: 56% (determined by NMR spectroscopy) orange solution, starting from **9b** dissolved in THF. ¹H NMR ([D₈]THF, 217 K): $\delta = 0.45$ (d, ³J(H, H) = 3.4 Hz, 6H; SiMe₂), 1.18 (s, 9H; *t*Bu), 4.58 (sept, 1H; SiH), 5.67 (s, 10H; Cp); ¹³C NMR ([D₈]THF, 217 K): $\delta = -0.7$ (SiMe₂), 32.8 (CMe₃), 41.9 (CMe₃), 106.6 (Cp), quart. C (alkyne) not observed; ²⁹Si NMR ([D₈]THF, 217 K): $\delta = -26.5$ (¹J(Si, H) = 174 Hz). IR (Nujol): $\tilde{\nu} = 2094 \text{ cm}^{-1}$ (SiH), 1688 cm⁻¹ (C≡C_{coord}).

[Cp₂Zr(*t*BuC₂SiMe₂H)] (9b): Yield: Method b) 68%, yellow-brown crystals, m.p. 87–92 °C. ¹H NMR (C₆D₆, 297 K): $\delta = -3.74$ (1H; SiH), 0.24 (d, ³J(H, H) = 1.7 Hz, 6H; SiMe₂), 1.50 (s, 9H; CH₃), 5.12 (s, 10H; Cp); ¹³C NMR (C₆D₆, 297 K): $\delta = -2.7$ (SiMe₂), 33.3 (CMe₃), 39.7 (CMe₃), 99.0 (CSiMe₂), 101.2 (Cp), 214.7 (CCMe₃); ²⁹Si NMR (C₆D₆, 297 K): $\delta = 16.1$ (¹J(Si, H) = 72 Hz). IR (Nujol): $\tilde{\nu} = 1689 \text{ cm}^{-1}$ (SiH, C≡C_{coord}). C₁₈H₂₆SiZr (361.7): calcd: C 59.77, H 7.25; found: C 59.55, H 7.61.

[Cp₂Zr(thf)(η^2 -PhC₂SiMe₂H)] (10a): Yield: Method b) 59% (determined by NMR spectroscopy), yellow-green. NMR ([D₈]THF at 213 K: two isomers, see Scheme 6): Major [minor] isomer, ¹H NMR: $\delta = 0.04$ [–0.06] (d, ³J(H, H) = 3.7 [3.6] Hz, 6H; SiMe₂), 4.44 [4.37] (sept, 1H; SiH), 5.80 [5.69] (s, 10H; Cp), 6.57–7.25 (Ph); ¹³C NMR: $\delta = -1.2$ [–1.3] (SiMe₂), 107.3 (Cp, both isomers), 122.3, 123.5, 123.8, 124.8, 127.8, 128.2, 152.3, 156.7, 165.0, 194.0, 199.3, 221.8 (C_q and CH); ²⁹Si: $\delta = -26.8$ [–22.2] (¹J(Si, H) = 176 [175] Hz). IR (Nujol): $\tilde{\nu} = 2064 \text{ cm}^{-1}$ (SiH), 1683 cm⁻¹ (C≡C_{coord}).

[Cp₂Zr(PhC₂SiMe₂H)] (10b): When **10a** was dissolved in toluene, **10b** was formed quantitatively, yellow solid, m.p. 78–84 °C. ¹H NMR ([D₈]toluene, 233 K): $\delta = -3.55$ (¹J(Si, H) = 73 Hz, 1H; SiH), 0.28 (d, ³J(H, H) = 1.9 Hz, 6H; SiMe₂), 5.00 (s, 10H; Cp), 7.20 (1H; *p*-Ph) 7.41 (2H; *m*-Ph), 8.27 (2H; *o*-Ph); ¹³C NMR ([D₈]toluene, 233 K): $\delta = -3.0$ (SiMe₂), 101.5 (Cp), 110.2 (CSiMe₂), 128.7, 129.1, 133.9 (CH Ph), 139.5 (*i*-Ph), 201.6 (CPh); ²⁹Si NMR ([D₈]toluene, 303 K): $\delta = 20.6$ (¹J(Si, H) = 88 Hz). IR (Nujol): $\tilde{\nu} = 1686 \text{ cm}^{-1}$ (SiH, C≡C_{coord}). C₂₀H₂₂SiZr (381.7): calcd: C 62.94, H 5.81; found: C 62.25, H 6.21.

[Cp₂Zr(thf)(η^2 -Me₃SiC₂SiMe₂H)] (11a): Yield: 63% (determined by NMR spectroscopy), yellow-brown solution, starting from **11b** dissolved in THF. ¹H NMR ([D₈]THF, 246 K): $\delta = 0.11$ (d, ³J(H, H) = 3.6 Hz, 6H; SiMe₂), 0.15 (s, 9H; SiMe₃), 4.54 (sept, 1H; SiH), 5.56 (s, 10H; Cp); ¹³C NMR ([D₈]THF, 246 K): $\delta = -1.1$ (SiMe₂), 2.0 (SiMe₃), 106.8 (Cp), quart. C (alkyne) not observed; ²⁹Si NMR ([D₈]THF, 246 K): $\delta = -23.6$ (¹J(Si, H) = 179 Hz; SiMe₂), -11.4 (SiMe₃).

[Cp₂Zr(Me₃SiC₂SiMe₂H)] (11b): Yield: Method a) 32%, yellow-brown crystals, m.p. 48–49 °C. ¹H NMR (C₆D₆, 297 K): $\delta = -4.29$ (1H; SiH), 0.33 (d, ³J(H, H) = 1.8 Hz, 6H; SiMe₂), 0.50 (s, 9H; SiMe₃), 5.05 (s, 10H; Cp); ¹³C NMR (C₆D₆, 297 K): $\delta = -2.7$ (SiMe₂), 1.4 (SiMe₃), 101.0 (Cp), 125.4 (CSiMe₂), 194.7 (CSiMe₃); ²⁹Si NMR (C₆D₆, 297 K): $\delta = -5.8$ (SiMe₃), 34.3 (¹J(Si, H) = 68 Hz; SiMe₂). C₁₇H₂₆Si₂Zr (377.8): calcd: C 54.05, H 6.94; found: C 53.79, H 6.62.

[Cp₂Zr(thf)(η^2 -HMe₂SiC₂SiMe₂H)] (12a): Yield: 57% (determined by NMR spectroscopy), orange-brown solution, starting from **12b** dissolved in THF. ¹H NMR ([D₈]THF, 203 K): $\delta = 0.08, 0.26$ (d, ³J(H, H) = 3.6 Hz, 6 H each; SiMe₂), 4.44, 4.74 (sept, 1 H each; SiH); 5.58 (s, 10H; Cp); ¹³C NMR ([D₈]THF, 203 K): $\delta = -1.1, -0.7$ (¹J(Si, C) = 49 and 50 Hz; SiMe₂), 77.7 (α -CH₂ THF), 106.8 (Cp), 198.3, 225.7 (¹J(Si, C) = 60 and 65 Hz; CSiMe₂); ²⁹Si NMR ([D₈]THF, 203 K): $\delta = -28.0, -21.3$ (¹J(Si, H) = 178 and 176 Hz).

[Cp₂Zr(HMe₂SiC₂SiMe₂H)] (12b): Yield: Method a) 70%, red-orange, m.p. 45 °C. ¹H NMR ([D₈]toluene, 246 K): $\delta = -4.40$ (1H; activated SiH), 0.24 (d, ³J(H, H) = 1.7 Hz, 6H; activated SiMe₂), 0.50 (d, ³J(H, H) = 3.7 Hz, 6H; SiMe₂), 4.93 (s, 10H; Cp), 5.05 (sept, 1H; SiH); ¹³C NMR ([D₈]toluene, 246 K): $\delta = -3.1$ (¹J(Si, C) = 66 Hz; activated SiMe₂), -1.5 (¹J(Si, C) = 52 Hz; SiMe₂), 100.8 (Cp), 127.1 (¹J(Si, C) = 59 Hz; activated CSiMe₂), 191.2 (¹J(Si, C) = 73 Hz; CSiMe₂); ²⁹Si NMR ([D₈]toluene, 246 K): $\delta = -21.6$ (¹J(Si, H) = 187 Hz), 35.3 (¹J(Si, H) = 69 Hz; activated SiH). C₁₆H₂₄Si₂Zr (363.8): calcd: C 52.83, H 6.65; found: C 53.12, H 6.59.

[Cp₂Ti–C(SiMe₂H)=CPh–C(SiMe₂H)=CPh] (13a): Yield: 28% (crystallization at –20 °C), brown crystals. ¹H NMR (C₆D₆, 297 K): $\delta = -0.25,$

–0.15 (d, $^3J(\text{H}, \text{H}) = 3.9$ and 3.8 Hz, 6 H each; SiMe_2), 3.14, 3.62 (sept, $^3J(\text{H}, \text{H}) = 3.8$ and 3.9 Hz, 1 H each; SiH), 6.01 (s, 10H; Cp), 6.92, 7.10, 7.42 (Ph); ^{13}C NMR (C_6D_6 , 297 K): $\delta = -1.0$, -0.6 (SiMe_2), 114.0 (Cp), 124.6, 126.2 (*p*-Ph), 125.4, 127.5, 127.9, 129.7 (CH Ph), 140.9, 146.7, 149.0, 149.6 (C_q), 211.1, 228.4 (CTi); ^{29}Si NMR (C_6D_6 , 303 K): $\delta = -29.6$ ($^1J(\text{Si}, \text{H}) = 189$ Hz), -36.3 ($^1J(\text{Si}, \text{H}) = 175$ Hz). Elemental analysis of a mixture of **13a** and **b**: $\text{C}_{30}\text{H}_{34}\text{Si}_2\text{Ti}$ (498.6): calcd: C 72.26, H 6.87; found: C 72.41, H 6.89.

[Cp₂Ti–C(SiMe₂H)=CPh–CPh=C(SiMe₂H)] (13b): Yield: 88% (crystallization at 0°C), brown prismatic crystals, m.p. 156–157°C. ^1H NMR (C_6D_6 , 297 K): $\delta = -0.15$ (d, $^3J(\text{H}, \text{H}) = 3.8$ Hz, 12H; SiMe_2), 3.31 (sept, 2H; SiH), 6.18 (s, 10H; Cp), 6.75 (4H; *o*-Ph), 6.77 (2H; *p*-Ph), 6.87 (4H; *m*-Ph); ^{13}C NMR (C_6D_6 , 297 K): $\delta = -1.1$ (SiMe_2), 113.8 (Cp), 125.4 (*p*-Ph), 127.1, 129.6 (CH Ph), 144.9, 150.0 (C_q), 218.1 (CTi); ^{29}Si NMR (C_6D_6 , 297 K): $\delta = -35.9$ ($^1J(\text{Si}, \text{H}) = 176$ Hz). IR (Nujol): $\tilde{\nu} = 2092$ cm^{-1} (SiH).

[Cp₂Zr–C(SiMe₂H)=CPh–C(SiMe₂H)=CPh] (14a): Yield: 40% (crystallization: one day at –30°C), orange. ^1H NMR ($[\text{D}_8]\text{toluene}$, 268 K): $\delta = -0.25$ (d, $^3J(\text{H}, \text{H}) = 4.0$ Hz, 6H; β - SiMe_2), -0.17 (d, $^3J(\text{H}, \text{H}) = 3.8$ Hz, 6H; α - SiMe_2), 3.56, 3.71 (sept, 1 H each; α - and β -SiH), 5.94 (s, 10H; Cp), 6.84 (2H; *o*- α -Ph), 6.88 (1H; *p*- α -Ph), 6.99 (1H; *p*- β -Ph), 7.06 (2H, *o*- β -Ph), 7.08 (2H; *m*- β -Ph), 7.11 (2H; *m*- α -Ph); ^{13}C NMR ($[\text{D}_8]\text{toluene}$, 268 K): $\delta = -1.6$, -0.2 (α -, β - SiMe_2), 111.9 (Cp), 123.9, 126.1 (*p* α -, β -Ph), 124.9, 128.9 (*o* α -, β -Ph), 128.2, 127.6 (*m* α -, β -Ph), 146.1, 148.2, 149.8, 156.5, 195.5, 222.9 (quart. C); ^{29}Si NMR ($[\text{D}_8]\text{toluene}$, 268 K): $\delta = -37.0$ ($^1J(\text{Si}, \text{H}) = 173$ Hz, α -Si), -29.4 ($^1J(\text{Si}, \text{H}) = 189$ Hz, β -Si). Elemental analysis of a mixture of **14a** and **b**: $\text{C}_{30}\text{H}_{34}\text{Si}_2\text{Zr}$ (542.0): calcd. C 66.48, H 6.32; found: C 66.35, H 6.27.

[Cp₂Zr–C(SiMe₂H)=CPh–CPh=C(SiMe₂H)] (14b): Yield: 76% (crystallization: 5 days at 0°C), yellow needles. M.p.: 160°C. ^1H NMR ($[\text{D}_8]\text{toluene}$, 268 K): $\delta = -0.19$ (d, $^3J(\text{H}, \text{H}) = 3.8$ Hz; 6H, SiMe_2), 3.70 (sept, 2H; SiH), 6.10 (s, 10H; Cp), 6.70 (4H; *o*-Ph), 6.71 (2H; *p*-Ph), 6.83 (4H; *m*-Ph); ^{13}C NMR ($[\text{D}_8]\text{toluene}$, 268 K): $\delta = -1.6$ (SiMe_2), 111.7 (Cp); 125.3, 127.1, 129.1 (*p*-, *m*-, *o*-Ph), 146.2 (*i*-Ph), 157.0 (CPh), 204.2 (CZr); ^{29}Si NMR ($[\text{D}_8]\text{toluene}$, 268 K): $\delta = -36.3$ ($^1J(\text{Si}, \text{H}) = 174$ Hz). IR (Nujol) $\tilde{\nu} = 2069$ cm^{-1} (SiH). MS(70 eV): *m/z*: 380 $[\text{M}]^+$.

Acknowledgments: We thank Prof. H. Günther and V. Francke, Siegen, for helpful discussions and assistance with the solid-state NMR spectra. Financial support by the Fonds der Chemischen Industrie, the Max-Planck-Gesellschaft, and the Stiftung Volkswagenwerk is gratefully acknowledged.

Received: February 27, 1998 [F 1032]

- [1] a) R. D. Miller, J. Michl, *Chem. Rev.* **1989**, *89*, 1359; b) *Silicon-Based Polymer Science*, Advances in Chemistry Series 224, (Eds.: J. M. Ziegler, F. W. G. Fearon), American Chemical Society, Washington, DC, **1990**.
- [2] R. West in *The Chemistry of Organic Silicon Compounds*, Vol. II (Eds.: S. Patai, Z. Rappoport), Wiley, New York, **1989**, Chapter 19.
- [3] C. Aitken, J. F. Harrod, E. Samuel, *J. Organomet. Chem.* **1985**, *279*, C11.
- [4] H. G. Woo, T. D. Tilley, *J. Am. Chem. Soc.* **1989**, *111*, 3757.
- [5] J. Y. Corey, X. H. Zhu, T. C. Bedard, L. D. Lange, *Organometallics* **1991**, *10*, 924; J. Y. Corey, X. H. Zhu, *Organometallics* **1992**, *11*, 672.
- [6] S. Bourg, R. J. P. Corriu, M. Enders, J. J. E. Moreau, *Organometallics* **1995**, *14*, 564.
- [7] T. D. Tilley, *Acc. Chem. Res.* **1993**, *26*, 22.
- [8] E. Hengge, M. Weinberger, *J. Organomet. Chem.* **1993**, *443*, 167.
- [9] J. F. Harrod, *ACS Symp. Ser.* **1988**, *360*, 89; J. F. Harrod, *NATO ASI Ser. E*, **1988**, *141*, 103.
- [10] J. P. Banovetz, K. M. Stein, R. M. Waymouth *Organometallics* **1991**, *10*, 3430; F. Gauvin, J. F. Harrod, *Can. J. Chem.* **1990**, *68*, 1638.
- [11] a) U. Schubert, *Adv. Organomet. Chem.* **1990**, *30*, 151; b) U. Schubert, G. Scholz, J. Müller, K. Ackermann, B. Wörle, R. F. D. Stansfield, *J. Organomet. Chem.* **1986**, *306*, 303.
- [12] C. Eaborn, P. N. Kapoor, D. J. Tune, C. L. Turpin, D. R. M. Walton, *J. Organomet. Chem.* **1973**, *63*, 323.
- [13] a) R. J. P. Corriu, J. J. E. Moreau, H. Praet, *Organometallics* **1990**, *9*, 2086; b) S. Kotani, T. Matsumoto, H. Yamaguchi, K. Shiina, K. Sonogashira, *Chem. Lett.* **1989**, 293.
- [14] A. Ohff, P. Kosse, W. Baumann, A. Tillack, R. Kempe, H. Görls, V. V. Burlakov, U. Rosenthal, *J. Am. Chem. Soc.* **1995**, *117*, 10399.
- [15] M. F. Fan, Z. Lin, *Organometallics*, **1997**, *16*, 494.
- [16] a) M. S. Eisen, *Rev. Inorg. Chem.* **1997**, *17*, 25; b) R. Beckhaus, *Nachr. Chem. Tech. Lab.* **1998**, *46*, 611.
- [17] L. J. Procopio, P. J. Carroll, D. H. Berry, *J. Am. Chem. Soc.* **1994**, *116*, 177.
- [18] R. Beckhaus, M. Wagner, V. V. Burlakov, W. Baumann, N. Peulecke, A. Spannenberg, R. Kempe, U. Rosenthal, *Z. Anorg. Allg. Chem.* **1998**, *624*, 129.
- [19] J. M. Manriquez, D. R. McAllister, R. D. Sanner, J. E. Bercaw, *J. Am. Chem. Soc.* **1976**, *98*, 6733.
- [20] C. P. Schaller, C. C. Cummins, P. T. Wolczanski, *J. Am. Chem. Soc.* **1996**, *118*, 591.
- [21] J. Yin, J. Klosin, K. A. Abboud, W. M. Jones, *J. Am. Chem. Soc.* **1995**, *117*, 3298.
- [22] M. Trommer, G. E. Miracle, B. E. Eichler, D. E. Powell, R. West, *Organometallics* **1997**, *16*, 5737.
- [23] E. Colomer, R. J. P. Corriu, C. Marzin, A. Vioux, *Inorg. Chem.* **1982**, *21*, 368.
- [24] V. B. Shur, V. V. Burlakov, M. E. Vol'pin, *J. Organomet. Chem.* **1988**, *347*, 77.
- [25] C. Lefeber, A. Ohff, A. Tillack, W. Baumann, R. Kempe, V. V. Burlakov, U. Rosenthal, H. Görls, *J. Organomet. Chem.* **1995**, *501*, 179.
- [26] V. V. Burlakov, A. Ohff, C. Lefeber, A. Tillack, W. Baumann, R. Kempe, U. Rosenthal, *Chem. Ber.* **1995**, *128*, 967.
- [27] U. Rosenthal, A. Ohff, W. Baumann, R. Kempe, A. Tillack, V. V. Burlakov, *Angew. Chem.* **1994**, *106*, 1678; *Angew. Chem. Int. Ed. Engl.* **1994**, *33*, 1605.
- [28] U. Rosenthal, C. Nauck, P. Arndt, S. Pulst, W. Baumann, V. V. Burlakov, H. Görls, *J. Organomet. Chem.* **1994**, *484*, 81.
- [29] A. Ohff, S. Pulst, C. Lefeber, N. Peulecke, P. Arndt, V. V. Burlakov, U. Rosenthal, *Synlett* **1996**, 111.
- [30] N. Peulecke, W. Baumann, R. Kempe, V. V. Burlakov, U. Rosenthal, *Eur. J. Inorg. Chem.* **1998**, 419.
- [31] a) U. Rosenthal, A. Ohff, W. Baumann, A. Tillack, H. Görls, V. V. Burlakov, V. B. Shur, *Z. Anorg. Allg. Chem.* **1995**, *621*, 77; b) U. Rosenthal, A. Ohff, M. Michalik, H. Görls, V. V. Burlakov, V. B. Shur, *Angew. Chem.* **1993**, *105*, 1228.
- [32] Known Zr–Si bond lengths range from 2.65 to 2.82 Å.^[20] For Ti–Si derivatives (2.60–2.67 Å) see: a) T. D. Tilley in *The Silicon-Heteroatom Bond Compounds* (Eds.: S. Patai, Z. Rappoport), Wiley, New York, **1991**, p 309 and references therein. Characteristic Zr–hydride distances were found at about 2 Å. Ti–H range between 1.66 and 1.97 Å for titanium hydride complexes; b) E. Spaltenstein, P. Palma, K. A. Kreutzer, C. A. Willoughby, W. M. Davis, S. L. Buchwald, *J. Am. Chem. Soc.* **1994**, *116*, 10308, and references therein.
- [33] The Si1–C11 distances of 1.787(3) Å (**12b**) and 1.766(7) Å (**1**) are between Si–C single bonds (1.87–1.91 Å^[33a]) and the C=Si double bond lengths in West's first stable silaallene (1.04 Å^[33b]), near to the region of η^2 -silene complexes (1.78–1.80 Å^[33c,d]). a) F. H. Allen, O. Kennard, D. G. Watson, L. Brammer, A. G. Orpen, R. Taylor, *J. Chem. Soc. Perkin Trans.* **1987**, 1–19; b) G. E. Miracle, J. L. Ball, D. R. Powell, R. West, *J. Am. Chem. Soc.* **1993**, *115*, 11598; c) T. S. Koloski, P. J. Carroll, D. H. Berry, *J. Am. Chem. Soc.* **1990**, *112*, 6405; d) B. K. Campion, R. H. Heyn, T. D. Tilley, *J. Am. Chem. Soc.* **1993**, *115*, 5527.
- [34] H. G. Woo, J. F. Harrod, E. Samuel, *Organometallics* **1993**, *12*, 2883.
- [35] E. D. Jemmis, K. T. Giju, *J. Am. Chem. Soc.* **1998**, *120*, 6952.
- [36] A. Tillack, C. Lefeber, N. Peulecke, D. Thomas, U. Rosenthal, *Tetrahedron Lett.* **1997**, *38*, 1533.
- [37] N. Peulecke, D. Thomas, W. Baumann, C. Fischer, U. Rosenthal, *Tetrahedron Lett.* **1997**, *38*, 6655.
- [38] G. Engelhardt, D. Zeigan, D. Hoebbel, A. Samoson, E. Lippmaa, *Z. Chem.* **1982**, *22*, 314.
- [39] G. M. Sheldrick, *Acta Crystallogr. A* **1990**, *46*, 467.
- [40] G. M. Sheldrick, Universität Göttingen, **1993**.